Journal of Nuclear Materials 381 (2008) 9–14

Contents lists available at ScienceDirect

Journal of Nuclear Materials

journal homepage: www.elsevier.com/locate/jnucmat

Comparison of the oxidation rate and degree of graphitization of selected IG and NBG nuclear graphite grades

Se-Hwan Chi *, Gen-Chan Kim

Nuclear Hydrogen Development and Demonstration Project, Korea Atomic Energy Research Institute (KAERI), 150 Dukjin-dong, Yuseong, Daejeon 305-353, Republic of Korea

A B S T R A C T

The oxidation rate and degree of graphitization (DOG) were determined for some selected nuclear graphite grades (i.e., IG-110, IG-430, NBG-18, NBG-25) and compared in view of their filler coke type (i.e., pitch or petroleum coke) and the physical property of the grades. Oxidation rates were determined at six temperatures between 600 and 960 °C in air by using a three-zone vertical tube furnace at a 10 l/min air flow rate. The specimens were a cylinder with a 25.4 mm diameter and a 25.4 mm length. The DOG was determined based on the lattice parameter *c* determined from an X-ray diffraction (XRD). Results showed that, even though the four examined nuclear graphite grades showed a highly temperature-sensitive oxidation behavior through out the test temperature range of 600–950 °C, the differences between the grades were not significant. The oxidation rates determined for a 5–10% weight loss at the six temperatures were nearly the same except for 702 and 808 °C, where the pitch coke graphites showed an apparent decrease in their oxidation rate, more so than the petroleum coke graphites. These effects of the coke type reduced or nearly disappeared with an increasing temperature. The average activation energy determined for 608–808 °C was 161.5 ± 7.3 kJ/mol, showing that the dominant oxidation reaction occurred by a chemical control. A relationship between the oxidation rate and DOG was not observed.

1. Introduction

Currently, a series of coordinated research and development studies on nuclear graphite are being performed in relation to the Generation-IV Very High Temperature Reactor (VHTR) collaboration plan for a nuclear graphite technology development. The basic idea that supports the coordinated research activities in Generation-IV member nations and their subordinate institutions is rather straightforward as described in the collaboration plan. Thus, to coordinate on the development of graphite data for several new grades of nuclear graphite together to support the design and construction of the structures associated with new Generation-IV reactor concepts [1].

In line with this idea, a series of R&D work is under way at the Korea Atomic Energy Research Institute (KAERI), a subordinate institute of a GIF member nation, Republic of Korea, under the frame work of the GIV graphite collaboration plan, including but not restricted to, a selection and qualification, a preparation of design data, and a machining of candidate graphite grades for the KAERI nuclear hydrogen development and demonstration (NHDD) project.

In the present study, in view of the selection and qualification of the candidate graphites, and the design data, the oxidation rate and degree of graphitization (DOG) were obtained and compared for four commercially available graphite grades, and the effects of the coke type on an oxidation and the dependency of an oxidation on the time and temperature, and the possible relationship between DOG and the oxidation rate were investigated.

2. Experimental

2.1. Materials and specimen

Four nuclear graphite grades, IG-110, IG-430, NBG-18 and NBG-25 were chosen for the present study by considering the manufacturing process (i.e., manufacturing process including the forming method), and the source of the coke, i.e., pitch or petroleum. Table 1 summarizes the characteristics of the grades. These graphites are being considered or being used, or have already been chosen for helium cooled high temperature gas reactors (HTGR) worldwide.

The specimen used for the present oxidation experiment was cylindrical with 25.4 mm in diameter and 25.4 mm in height. Specimens were machined by using a computerized numerical control (CNC) lathe with a poly-crystal diamond (PCD) bite at 1200 rpm. No further specimen surface treatments were applied after a specimen machining.

Powder samples for the lattice parameter (*c*) determination by XRD were prepared by pulverizing an amount of a sample taken from each graphite in an agate mortar and pestle, of which all

* Corresponding author.
E-mail address: shchi@kaeri.re.kr (S.-H. Chi).

0022-3115/$ - see front matter © 2008 Elsevier B.V. All rights reserved.
doi:10.1016/j.jnucmat.2008.07.027

Table 1
Characteristics of four commercially available nuclear graphite chosen for the present study[a]

Grade	Manufacturer	Forming method	Source coke	Grain size (μm)	Ash content (ppm)	Density (g/cm^3)
IG-110	Toyo Tanso	Iso-stat. molded	Petroleum	~20: fine-grain	<10	1.77
IG-430	Toyo Tanso	Iso-stat. molded	Coal	~10: fine-grain	<10	1.82
NBG-18	SGL	Vibra. molded	Coal	~300: med-grain	<10	1.85
NBG-25	SGL	Vibra. molded	Petroleum	~300: med-grain	<11	1.82

[a] All the values cited in the Table 1 are nominal values from the manufacturer's report.

had been passed through a 150 mesh standard sieve (the particle size is less than 100 μm). The pulverized graphite powder samples were mixed with 20 wt% standard silicone (size: 4.9 μm, SEM640C, NIST) as an internal standard [2].

2.2. Determination of oxidation rate

2.2.1. Oxidation test system

Oxidation rate was determined by using a graphite oxidation test system which was composed of a vertical tube furnace, 3-zone furnace controller, a gas supplier, and an analytical balance (capacity: 200 g, resolution: 0.001 g), as shown Fig. 1. The test system was manufactured by the draft ASTM Standard Test Method for Oxidation Rate and Threshold Oxidation Temperature for Manufactured Carbon and Graphite in Air [3]. The system was designed to control the specimen temperature below ±2 °C at 750 °C, and capable of 1150 °C with a Kanthal heating element. The gas supplier was composed of a flow meter, a desiccant column both for dry air and nitrogen gas (<0.005 mg water/l at 25–30 °C), an oxygen trap for Nitrogen gas, and flow meters for N_2, and air. Highly purified N_2 gas (99.999%) and dry air were used. During a test, a flow rate of a minimum of 10 l/min was maintained, and an automated data collection system was used to record the logged specimen weight and temperature data until the specimen had lost about 10% of its initial weight.

2.2.2. Determination of kinetics: oxidation rate (OR), activation energy (AE), and frequency factor (FF)

ORs were determined at six temperatures, i.e., 603, 702, 808, 854, 911 and 953 °C, and the AE and FF were determined for 603–808 °C.

These temperatures were chosen to investigate the oxidation characteristics of the grades within the chemical and in-pore diffusion or boundary layer controlled regime [4]. It is known that the OR in this regime is highly dependent on the internal-microstructure of a graphite [5–8].

In the present study, weight-loss data stored in an automated data collection system was used to characterize the oxidation properties of the selected grades by their weight loss (%)-time behavior, OR – time and OR – temperature behavior, AE, and the pre-exponential factors of the Arrhenius plot for an AE determination. The linear rate of the weight loss between 5% and 10% of the specimen's initial weight was used for a determination of the OR at four oxidation temperatures in units of g h^{-1} m^{-2}. AE was determined in units of kJ/mol from the slope of ln (oxidation rate) vs. T^{-1}, and the FF (A) from Rate $= Ae^{-E_a/RT}$, where E_a is AE, R is a universal gas constant and T is the reaction temperature. Further treatment of the kinetics and the theoretical value of the FF are reported elsewhere [3,9].

2.3. Determination of degree of graphitization (DOG) from lattice parameter c

The DOG ($\bar{g}$) was determined from c by referring to the procedure explained in Ref. [10], where $d(002) = c/2 = 3.354$ Å for $\bar{g} = 1$ and $d(002) = 3.44$ Å for $\bar{g} = 0$, and the lattice parameter c was obtained by referring to the Japanese procedure for measurements of the lattice parameters and the crystallites sizes of carbon materials by an X-ray diffraction [11].

Here, the DOG was determined as follows:

$$\bar{g} = \frac{[3.440 - d(002)]}{[3.440 - 3.354]}. \quad (1)$$

Table 2 summarizes the condition for the X-ray diffraction (Model: Rigaku D/Max 2500 V).

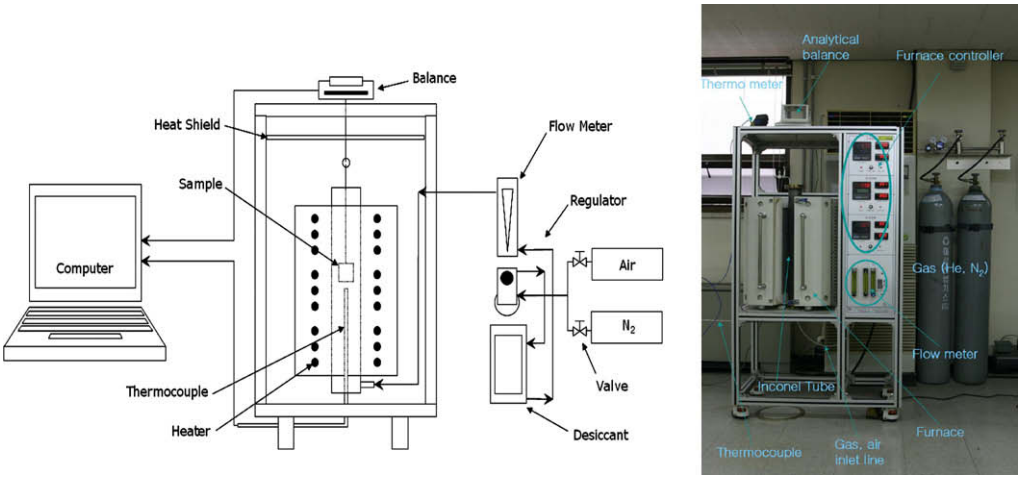

Fig. 1. Graphite oxidation test system manufactured to satisfy the requirement of (draft) ASTM Standard Test method for oxidation rate for manufactured carbon and graphite in air.

Table 2
Condition for the X-ray diffraction used in the present study for the lattice parameter measurement

	Condition		Condition
X-ray	Cu/40 kV/100 mA	Receiving slit	0.15 mm
Goniometer	RINT 2000 vertical goniometer	Monochromator receiving slit	No use
Attachment	Standard sample holder	Counter	Scintillation counter
Filter	Unused	Scan mode	Continuous
Instant monochromator	Unused	Scan speed	10.000°/min.
Counter monochromator	Fixed Monochromator	Sampling width	0.040°
Divergence slit	1°	Scan axis	2 theta/theta
Divergence height-limiting slit	10 mm	Scan range	10.000 → 90.000°
Scattering slit	1°	Theta offset	0.000°
Wavelength	1.54056 Å		

3. Results

3.1. Oxidation behavior

3.1.1. Weight loss behavior

Figs. 2–5 show the weight loss (%) versus the time behavior of the samples at 603 °C (Fig. 2), 702 °C (Fig. 3), 808 °C (Fig. 4), and 911 °C (Fig. 5), respectively, and Fig. 6 shows the optical photos of the four nuclear graphite grade samples oxidized at 808 °C in dry air (weight loss: 10%, flow rate: 10 l/min).

Firstly, Figs. 2 and 3 show that, the weight loss behavior appeared to be different according to the source coke type. In these temperatures, the grades made of petroleum coke, i.e., NBG-25 and IG-110, clearly show a faster weight loss behavior than the grades made of pitch cokes, i.e., NBG-18 and IG-430. The difference according to the coke appeared to disappear with an increase in the oxidation temperature, Figs. 4 and 5. Fig. 4 (808 °C) shows a clear difference in the weight loss behavior between the grades in the early stage of an oxidation. The order of the weight loss with time is clear. Thus, in a descending order, IG-110 > NBG-25 > IG-430 > NBG-18. It is seen in Fig. 5 that the clear differences in the weight loss behavior between the grades that appeared in Figs. 2–4 decreased or almost disappeared. From the comparison between Figs. 4 and 5, it is predicted that a change in the weight loss mechanism during an oxidation may have occurred between these temperatures.

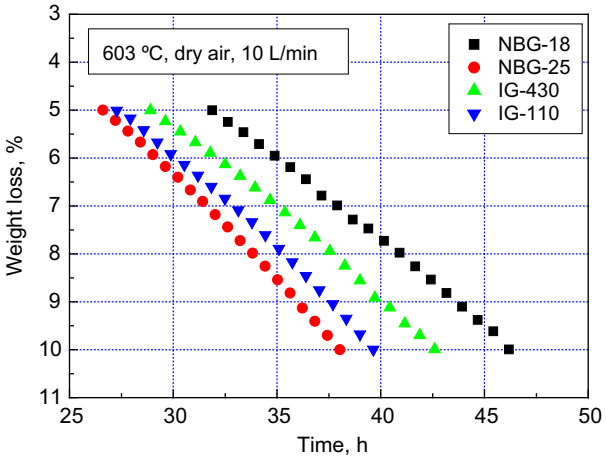

Fig. 2. Weight loss (%) behavior of four nuclear graphite grades (NBG-18, NBG-25, IG-110, IG-430) in dry air (603 °C, flow rate: 10 l/min).

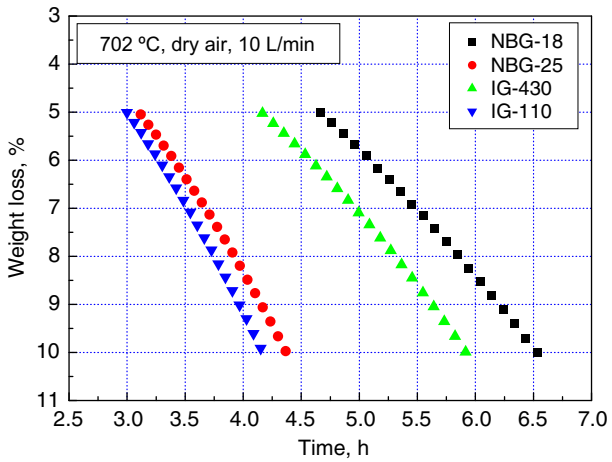

Fig. 3. Weight loss (%) behavior of four nuclear graphite grades (NBG-18, NBG-25, IG-110, IG-430) in dry air (702 °C, flow rate: 10 l/min).

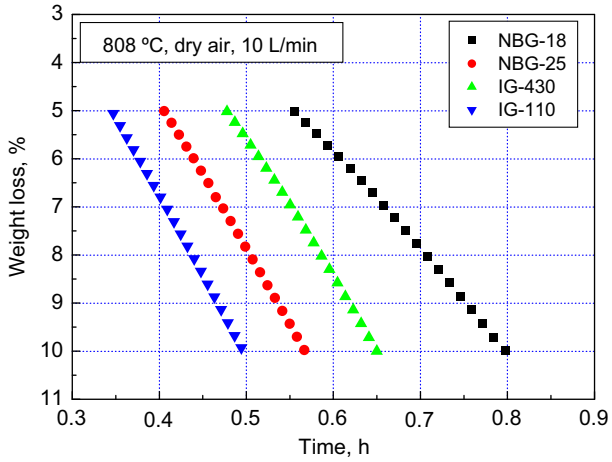

Fig. 4. Weight loss (%) behavior of four nuclear graphite grades (NBG-18, NBG-25, IG-110, IG-430) in dry air (808 °C, flow rate: 10 l/min).

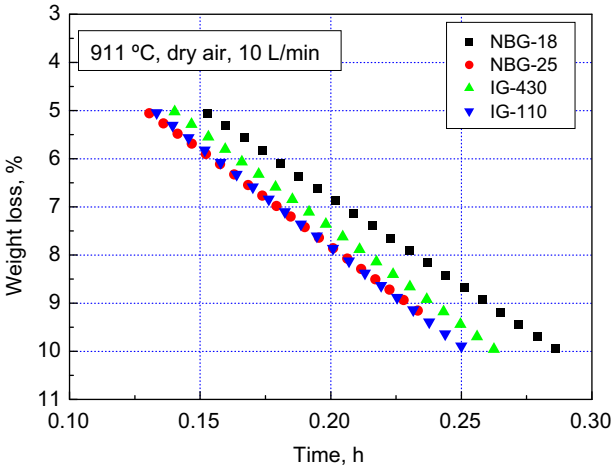

Fig. 5. Weight loss (%) behavior of four nuclear graphite grades (NBG-18, NBG-25, IG-110, IG-430) in dry air (911 °C, flow rate: 10 l/min).

Fig. 6. The optical photos of the graphite specimens oxidized at 808 °C in dry air at a flow rate of 10 l/min (weight loss: 10%).

3.1.2. Oxidation rate behavior

3.1.2.1. Oxidation rate (OR) change with the temperature. Changes of the OR upon an oxidation temperature are summarized in Fig. 7 and Table 3, respectively. While the increase in the OR from 603 to 702 °C is not significant, it shows a drastic increase from 702 to 854 °C. From 854 to 911 °C, no large change in the OR is observed. Even a little decrease in the OR is observed for the three grades except for NBG-18. Thus, all the grades except for NBG-18 show a little decrease in the OR with an increasing temperature. At 911 °C, all four grades show an increase in the OR. It is worth noting that NBG-18 consistently shows a minimum value in the OR through out all the test temperatures.

If compared, the oxidation rates at 854 °C are roughly 10–14 times higher than the rates at 702 °C.

It is worth noting that, at 911 and 953 °C, the differences in the oxidation rates between the grades are negligible.

Fig. 8 shows, for NBG-25 as an example, the changes in the oxidation rate upon the time before they reach a steady-state, stabilized oxidation rate at each test temperature. Clear differences in the modes of an oxidation rate increase are observed for the test temperatures.

While the oxidation rate reaches a steady-state (i.e., saturation) oxidation rate value (3100 g h^{-1} m^2) within 3 min at 911 °C, and about 30 min at 808 °C, in the case of 603 and 702 °C, no steady-state oxidation rate was observed even after about 40 h both at 603 and 702 °C. The mode of the increase in the OR at 808 °C appeared as a mixed form of two curves at 603 (702) °C and 911 °C.

3.1.2.2. Oxidation rate change with the time at 808 °C and 911 °C. Fig. 9(a) and (b) shows the changes of the oxidation rate upon the time at 808 °C and at 911 °C, respectively. The four grades show a large difference in the OR with time before they reach steady-state oxidation rates. It is worth noting that, while the three grades except for NBG-18 reach a similar steady-state oxidation rate of 2500 g h^{-1} m^2 between 0.4 and 0.8 h, the NBG-18 had not reached a steady-state oxidation rate as shown in Fig. 9(a). The grades reach a steady-state OR in a descending order IG-110 > NBG-25 > IG-430 > NBG-18.

In Fig. 9(b), little differences are observed in the increasing behaviors of the OR and in the steady-state OR values except for NBG-18. The NBG-18 showed the smallest oxidation rates both in

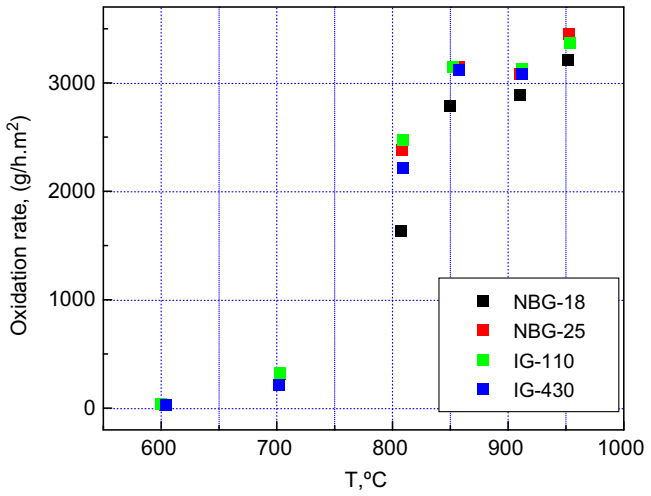

Fig. 7. Effects of the temperature on the oxidation rates of four samples. The oxidation rates in this figure were obtained from about a 5–10% weight loss regime (i.e., at a range of a steady-state oxidation rate) at each temperature.

Table 3
Oxidation rates of the grades at 603, 702, 808, 854, 911 and 953 °C

Graphite	Oxidation rate (g h^{-1} m^2)					
	603 °C	702 °C	808 °C	854 °C	911 °C	953 °C
NBG-18	27.1	211.1	1634.2	2782.9	2889.5	3209.2
NBG-25	33.8	301.2	2380.3	3150.0	3078.9	3446.1
IG-430	28.3	215.4	2214.5	3114.5	3078.9	3339.5
IG-110	30.4	322.6	2475.0	3150.0	3126.3	3363.2

The values in this table were obtained from about a 5–10% weight loss regime (i.e., at a range of steady-state oxidation rate) at each temperature.

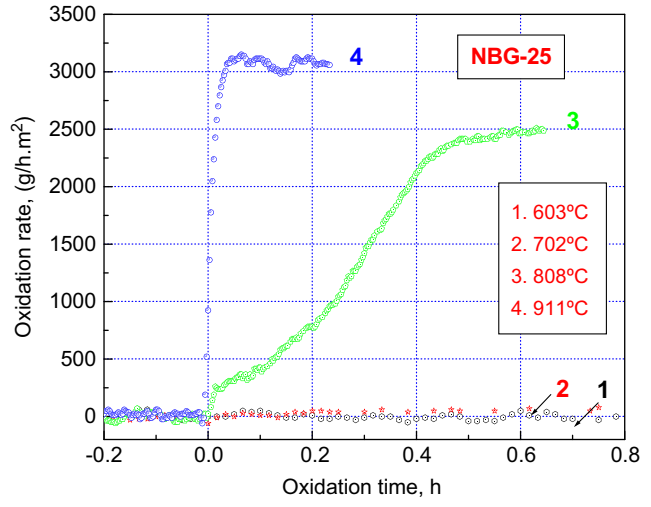

Fig. 8. Three modes of the increase in the oxidation rate with time for the test temperature (NBG-25).

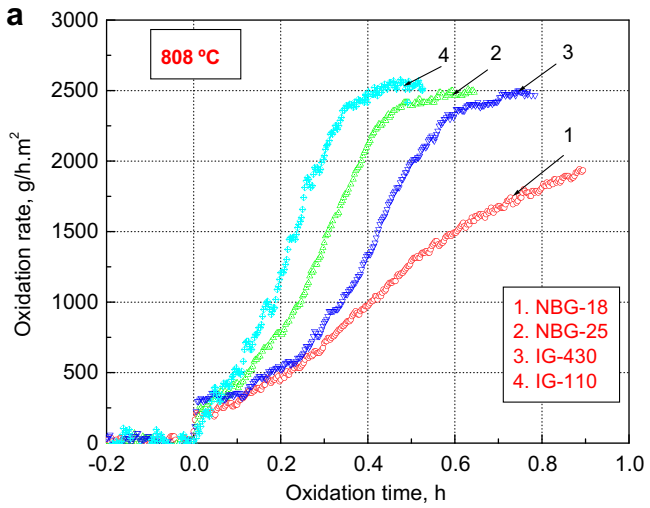

Fig. 9. Oxidation rate change with time at 808 °C (a) and at 911 °C (b).

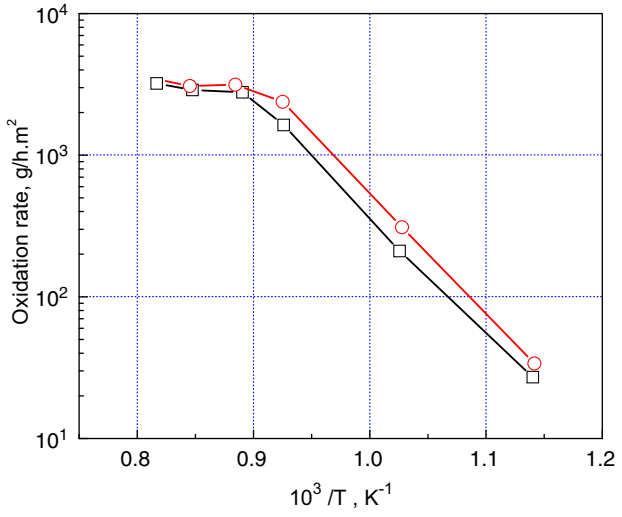

Fig. 10. Arrhenius plots for activation energy determination for 603–808 °C.

Fig. 9(a) and (b). From the differences in the oxidation time for reaching a steady-state OR between Fig. 9(a) (>0.4 min) and (b) (<0.1 min), a clear difference in the oxidation kinetics may be confirmed between 808 and 911 °C.

Table 4
Activation energies and pre-exponential factors determined for the temperature range of 603–808 °C

Graphite	E_a (kJ/mol)	Frequency factor (g h^{-1} m^2) × 10^{11}
NBG-18	157.1 ± 6.9	0.60 ± 0.02
NBG-25	163.1 ± 4.9	1.75 ± 0.04
IG-430	167.4 ± 12.4	2.44 ± 0.14
IG-110	158.9 ± 4.8	1.11 ± 0.03

Table 5
Summary of the lattice parameter (c) and degree of graphitization (DOG)

Grade	Lattice parameter (c) (Å)	Degree of graphitization ($\bar{g}$)
IG-110	6.73421	0.84762
IG-430	6.73471	0.84471
NBG-18	6.73646	0.83453
NBG-25	6.74423	0.78937

3.2. Activation energy

The Arrhenius plots for an activation energy determination for 603–808 °C are seen in Fig. 10. Determined activation energies are summarized in Table 4. No large differences between the grades are noted for the activation energy. The average activation energy of the four grades was 161.5 ± 7.3 kJ/mol. A gradual change in the slope between 808 and 854 °C (i.e., decrease in the activation energies) was noted. The activation energies and pre-exponential factors determined for the temperature range, i.e., 603–808 °C, are summarized in Table 4.

3.3. Lattice parameter (c) and degree of graphitization (DOG)

Table 5 summarizes the lattice parameter (c) and DOG from the XRD [12]. It is shown that the lattice parameter (c) is the largest for NBG-25, and the differences between the grades are not significant. Resultantly, the DOG of the grades was nearly the same for them all.

4. Discussion

Figs. 2 and 3 show a clear effect of the coke type on the weight loss behavior during an oxidation in air especially at 603 and 702 °C irrespective of the manufacturing process (thus, raw materials and manufacturing process) in that the weight loss behavior is different by the type of coke used and the graphite made of pitch coke shows a higher resistant to an oxidation than the graphite made of petroleum coke for both temperatures. From the observation that a distinct materials characteristic (i.e., coke type) appeared in the weight loss behavior during an oxidation, the oxidations at these two temperatures are assumed to have occurred by a mechanism greatly affected by the characteristics of the materials; i.e, chemical reaction [4,13].

Of these four grades, the NBG-18 of pitch coke showed the least oxidation rate through out the six oxidation temperatures (Table 3). The present observation for NBG-18 may be attributed to the highest density, the largest grain size, the lowest frequency factor and the lowest open pore density of the grades in a comparison to the other three grades, Table 1 and Ref. [14]. In addition, a higher density and a larger size of the Mrozowski cracks observed in the petroleum coke graphite may also have contributed to the present observation [15,16]. Regarding the frequency factor, it is known

that the lower the frequency factor, the lower the reaction opportunities per unit time [9].

The apparent effects of the coke type observed at 603 and 702 °C seem to be reduced or nearly disappeared at 808 and 911 °C. It is understood that the oxidation reactions are largely controlled by material-specific factors at 603 and 702 °C, and these dominant controlling factors are replaced by non-material-specific factors, i.e., such as a diffusion or supply of an oxidant, at 808 and 911 °C [3,4]. The fact that the changes in the dominant controlling factors have occurred for 808–911 °C is reflected well in Fig. 7 as changes in the oxidation rate and changes in the slope at around 808–854 °C in Fig. 10, respectively. It is worth noting that the decrease in the activation energy from above 808 °C is coincident with the assumed change in the oxidation mechanism from a material-dependent to a non-material-dependent mechanism in Fig. 10 [17]. Further it is noted that the temperature at which large differences between the grades are observed for the oxidation rate is 808 °C as seen in Figs. 4, 7 and 9(a) and Table 3. It is interesting to note that this temperature belongs to a temperature range where distinct material characteristics are reflected, Figs. 6 and 9(a).

In Table 3, a comparison of the oxidation rate between 808 and 953 °C shows that the temperature-dependency of the graphite oxidation is quite high, revealing that the oxidation mechanism of the graphite changes with the temperature, and the dependency of a graphite oxidation on an oxidation mechanism is critical, as confirmed by Figs. 8 and 9, where an apparent difference in the oxidation mechanism with the temperature is confirmed.

Regarding the dominant oxidation mechanism change at around 808–854 °C, the activation energy determined for 603–808 °C, 161 kJ/mol, and Fig. 6 of the oxidized specimen at 808 °C (10% weight loss) show that an oxidation occurs by a chemical control to a lesser extent from a boundary layer control [4].

Finally, regarding the relationship between the DOG and oxidation rate, no relationship may be assumed since the NBG-18 of the highest oxidation resistance shows the lowest DOG (even the differences between the grades is not large), Tables 3 and 5, suggesting that no reliable prediction may be made on the oxidation behavior of a grade based only on the DOG.

5. Conclusion

While the four examined nuclear graphite grades showed a highly temperature-sensitive behavior through out the test temperature range of 600–950 °C, differences between the grades were not significant. Thus, over all, the four nuclear grades from the NBG and IG grades showed a similar oxidation behavior. The oxidation rates determined for a 5–10% weight loss at the six temperatures were nearly the same except for 702 and 808 °C, where the pitch coke graphites showed a smaller oxidation rate than the petroleum coke graphites. These effects of the coke type reduced or disappeared with an increasing temperature. The average activation energy determined for 608–808 °C was 161.5 ± 7.3 kJ/mol, showing that the dominant oxidation reaction occurred by a chemical control. No relationship was found between the oxidation rate and DOG.

Acknowledgements

The authors wish to acknowledge Messrs B.J. Kim and J.H. Chang for their help through out the oxidation experiments, and SGL and Toyo Tanso for providing us NBG and IG grade samples, respectively. This work has been carried out as a part of Nuclear Hydrogen Development and Demonstration (NHDD) project in Korea Atomic Energy Research Institute (KAERI). Financial supports from Ministry of Education, Science and Technology (MEST) are acknowledged.

References

[1] Generation-IV International Forum, Project Management Board-VHTR/Materials and Components, Collaboration Plan for Graphite Technology Development Area (Draft). GIF Technical Secretariat, June 2006.
[2] Jane Howe, Plan on the ASTM XRD Round Robin on Graphitic Carbon Materials (Updated on 02/18/2005).
[3] C.I. Contescu, F.S. Baker, T.S. Burchell, in: Proceedings of the International Carbon Conference, Aberdeen, Scotland, 16–24 July, 2006.
[4] A. Blanchard, The Thermal Oxidation of Graphite, Appendix 2 (IAEA-TECDOC-1154, p. 211).
[5] V.Zh. Shemet, A.P. Pomytkin, V.S. Neshpor, Carbon 31 (1993) 1.
[6] E. Loren Fuller, Josef M. Okoh, J. Nucl. Mater. 240 (1997) 241.
[7] A.K. Bhattacharya, P. Bandopadhyay, P. Das, Ceram. Int. 29 (2003) 967.
[8] M. Balden, K.U. Klages, W. Jacob, J. Roth, J. Nucl. Mater. 341 (2005) 31.
[9] F. Stevens, L.A. Kolodny, T.P. Beebe Jr., J. Phys. Chem. B102 (1998) 10799.
[10] M.S. Seehra, A.S. Pavlovich, Carbon 31 (1993) 557.
[11] N. Iwashita, Chong Rae Park, H. Fujimoto, M. Shiraishi, M. Inagaki, Carbon 42 (2004) 701.
[12] Eun-Kyung Choi, Se-Hwan Chi, in: Proceedings of the Korean Carbon Society Spring Meeting, Keumho National Institute of Technology, Gumi, Gyeongbuck, Korea (in Korean), 18–19 May 2006, p. 53.
[13] L.E. Cascarini de Torre, J.L. Llanos, E.J. Bottani, Carbon 29 (1991) 1051.
[14] Gen-Chan Kim, Se-Hwan Chi, in: Transactions of the Korean Nuclear Society Spring Meeting, Chuncheon, Korea, 25–26 May, 2006.
[15] Se-Hwan Chi, Gen-Chan Kim, Jonghwa Chang, in: INGSM-6, Chamonix 2005, 18-21 October 2205, Chamonix, France, 2005;
Se-Hwan Chi, Gen-Chan Kim, in: Proceedings of Korean Nuclear Society 2006 Spring Meeting, Chuncheon, Korea, May, 25-26, 2006.
[16] Se-Hwan Chi, Gen-Chan Kim, Jong-Hwa Chang, in: Proceedings of ICCAP'2006, June 4–8, 2006, Reno, Nevada, USA, p. 2142.
[17] Luo Xiaowei, Robin Jean-Charles, Yu Suyuan, Nucl. Eng. Des. 227 (2004) 273.